

# Chapter 16

## Antimicrobial Nanomaterials for Water Disinfection

Chong Liu, Xing Xie, and Yi Cui

### 16.1 Introduction

To date, outbreaks of water-borne diseases, caused by pathogens, still occur at unexpectedly high levels, and they remain the leading cause of death in many developing countries. Worldwide, over one billion people lack reliable access to clean water, and water contamination causes two million deaths annually [1–3]. In addition, many people in the world live in water-stressed areas, and this number has kept on increasing over the last few years, which makes natural water disinfection and wastewater recycling and purification technologies urgently needed. Water disinfection and purification, the last procedure is to remove contaminated pathogens from drinking water, is critical for ensuring public health, and its importance can never be overemphasized.

Commonly, water treatment methods are based on two strategies, removing contaminated pathogens or inactivating them. Traditionally used water treatment methods include: size exclusion, chlorine disinfection, ozone disinfection, and UV disinfection. The use of size-exclusion membranes to remove bacteria is very effective and is not limited to certain kinds of pathogens. Even when the sizes of the microorganisms are very small, like some viruses, membrane filtration can also be quite effective by decreasing the pore sizes. However, the low treatment speed and high energy consumptions by using high pressures, limit its application. Chlorine disinfection is the most popular method for water treatment. However, research has revealed that, while increasing the efficiency of disinfection, the amount of harmful disinfection by-products (BDPs) is also increasing. Chemical

---

C. Liu • Y. Cui (✉)

Material Science and Engineering, Stanford University, Stanford, CA, USA

e-mail: [yicui@stanford.edu](mailto:yicui@stanford.edu)

X. Xie

Civil and Environmental Engineering, Stanford University, Stanford, CA, USA

disinfectants such as free chlorine, chloramines and ozone can react with various content in natural water to form carcinogenic DBPs [4]. In addition, chlorine disinfection can cause unpleasant tastes and odors. UV disinfection has drawn more attention in recent decades because of its high efficiency and ease of use. However, the disinfection set-up is very expensive and the UV lamp needs to be changed frequently. Hence, there is an urgent need for innovative, low cost and high efficiency water treatment methods.

Recently, nanotechnology has opened an alternative way for water disinfection. Nanomaterials' high surface-to-volume ratios, crystallographic structure, and adaptability to various substrates increase their contact efficiency with contaminated pathogens and hence result in more effective inactivation [5]. Several natural and engineered nanomaterials have been demonstrated to have strong antimicrobial properties through diverse mechanisms. In this chapter, we will discuss some of the most popular nanomaterials used for disinfection. And based on recent work in this area, we will further discuss the disinfection mechanisms of these nanomaterials.

## 16.2 Antimicrobial Nanomaterials

Nanomaterials are usually defined as any materials smaller than one-tenth of a micrometer in at least one dimension. To date, several antimicrobial nanomaterials have been applied to water disinfection. They can be classified into three main categories: (1) oligodynamic metals, including silver (Ag), copper (Cu), zinc (Zn), titanium (Ti), and cobalt (Co) [6]; (2) photocatalytic semiconductors, including  $\text{TiO}_2$ , ZnO, and  $\text{WO}_3$  [7, 8]; and (3) carbon nanomaterials, including carbon nanotubes and fullerenes [9–11]. These nanomaterials can potentially be used as alternative disinfectants or coupled with current technologies to enhance the inactivation efficacy. In the following part of this section, we will briefly introduce the mechanisms of these nanomaterials used for water disinfection, and then mainly discuss how these nanomaterials are currently applied for water disinfection and what the advantages and disadvantages are of using these antimicrobial nanoparticles.

### 16.2.1 *nAg*

Silver is the most widely used oligodynamic metal for water disinfection, due to its wide range of antimicrobial effect, low toxicity to humans, and ease of operation [6]. The antimicrobial properties of silver have been known for centuries. Many examples of using silver to kill pathogens or prevent microbial growth can be found in history all over the world. To prevent water-borne diseases, people have used silver vessels to store water or have put silver coins in their barrels [12].

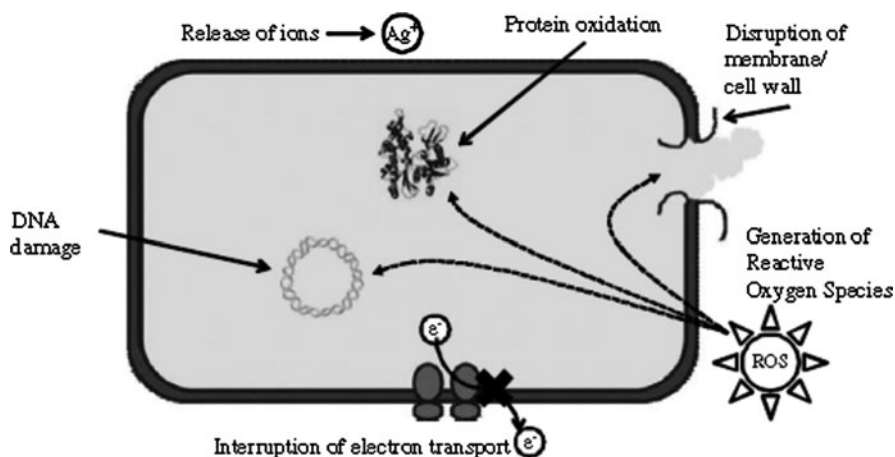
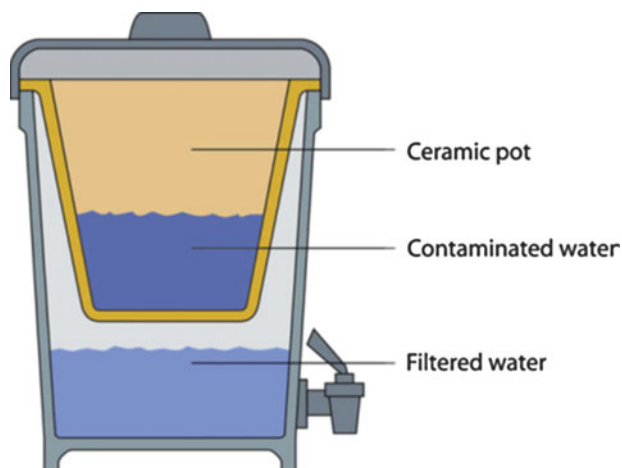


Fig. 16.1 A schematic of the possible mechanisms of antimicrobial activity of silver [4]

The antimicrobial effect of silver ions has been published many times in the literature and may include the following mechanisms: (1) interact with thiol groups and inactivate critical enzymes; (2) interact with DNA and prevent DNA replication; (3) catalyze the generation of reactive oxygen species (ROS); (4) change the permeability of the cell membrane; and (5) interrupt the electron transport [4, 6, 13–16]. Silver nanomaterials can disrupt the cell wall and penetrate through the cell membranes themselves, or they can kill the pathogens by releasing silver ions [4]. A schematic summarizing the possible mechanisms is shown in Fig. 16.1 [4]. Smaller silver particles, less than 10 nm, are more toxic, because smaller particles are able to more easily penetrate the cell membranes [16–18]. Furthermore, triangular silver nanoplates containing more {111} surface were found to be more toxic than nanorods, nanospheres, or silver ions [16, 17].

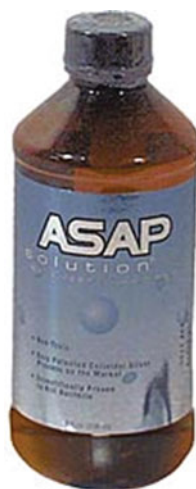
Silver disinfection is very promising for point-of-use (POU) application. One example, which has actually been commercialized and is widely used in many developing countries, is the silver nanoparticle-embedded ceramic filter, as shown in Fig. 16.2 [19–24]. Silver disinfectant products can also be found online when you are preparing an emergency package, such as the one called ASAP Silver Solution shown in Fig. 16.3. Large-scale applications are still under study. The most common idea is immobilizing silver nanomaterials on some porous substrate, such as various membranes and even paper [25–30]. Figure 16.4 shows a section of fiberglass impregnated with silver nanoparticles used for water filters [25].

Several issues need to be considered for water disinfection using silver nanomaterials. First, the antimicrobial effect of silver nanomaterials is caused by both direct contact and irreversibly releasing silver ions. Small particle size with big surface–volume ratio will enhance the inactivation efficacy, but it will also increase the rate of loss of silver. Therefore, it is very challenging to control the releasing rate of silver ions to have both a long life time and a sufficient killing effect. Secondly, a high concentration of silver in the treated water is also harmful to



**Fig. 16.2** A schematic of the silver nanoparticle-embedded ceramic pot [21]

**Fig. 16.3** A bottle of ASAP silver solution (beprepared.com)



human health [31]. The U.S. Environmental Protection Agency (EPA) mean contamination level (MCL) for silver in drinking water is 0.1 mg/L [32]. Lastly, it has been reported that some microbes have been shown to be resistant to silver [33].

### 16.2.2 $TiO_2$

$TiO_2$  is the most commonly used photocatalyst. It is the most studied nanomaterial for water disinfection, although it has only been used for killing microbes for about 30 years [34]. The mechanisms of the antimicrobial effect of  $TiO_2$  are mainly

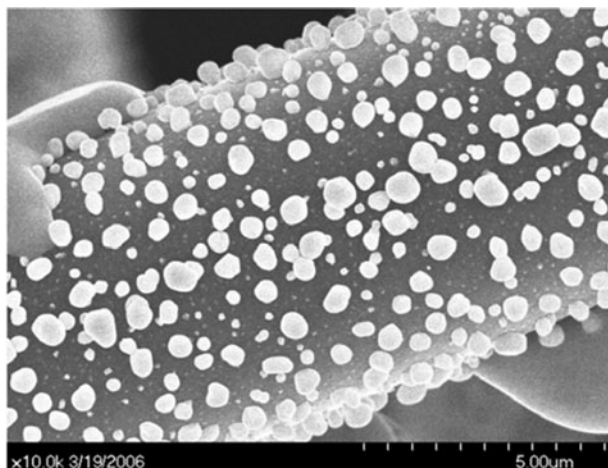


**Fig. 16.4** SEM image of a silver nanoparticle impregnated fiberglass [25]

related to the generation of ROS, especially hydroxyl free radicals and peroxide, under UV-A irradiation ( $300 \text{ nm} < \lambda < 390 \text{ nm}$ ) [7, 35]. Antimicrobial effect was also reported in the dark condition, indicating other non-photo-related mechanisms [36]. It has been reported that anatase phase  $\text{TiO}_2$  showed higher photocatalytic activity than the rutile phase [37]. Doping with noble metals, especially silver, can increase the photocatalytic activity and extend the active absorption to visible light [38, 39]. Depending on the particle size and the intensity of the light, the normally used concentration of  $\text{TiO}_2$  varies between 100 and 1,000 mg/L [40].

$\text{TiO}_2$  also has potential to be used in POU disinfection, because its photocatalytic activity can enhance solar disinfection [41, 42]. Figure 16.5 shows a photograph of a POU  $\text{TiO}_2$ -assisted solar disinfection system called the SOLWATER and AQUACAT system [42]. Water from the feed tank is pumped through illuminated tubes connected in series in a compound parabolic concentrator solar collector. Electricity is provided by a solar panel on the right, as shown in the figure. However, solar disinfection usually requires long reaction times. In these applications, doping is critical to enhance the absorption of visible light to shorten the reaction time [4].

Many  $\text{TiO}_2$ -based photocatalytic reactors have been studied, such as the annular slurry photoreactor (Fig. 16.6) [43], flow-through photoreactor (Fig. 16.7) [44], cascade photoreactor (Fig. 16.8) [45], etc. Although some of these reactors have been applied for treating organic contaminants, they can also be used for water disinfection. These reactors can be classified into two main configurations: (1)  $\text{TiO}_2$  catalysts are suspended in the reactor; and (2)  $\text{TiO}_2$  catalysts are immobilized onto an inert substrate [7].

To date, type 1 reactors are still preferred, due to the high total surface area of the  $\text{TiO}_2$  per unit volume and the ease of the photocatalyst reactivation [7]. However, an additional downstream separation unit to recover the  $\text{TiO}_2$  nanoparticles is required



Fig. 16.5 SOLWATER and AQUACAT solar disinfection system [42]

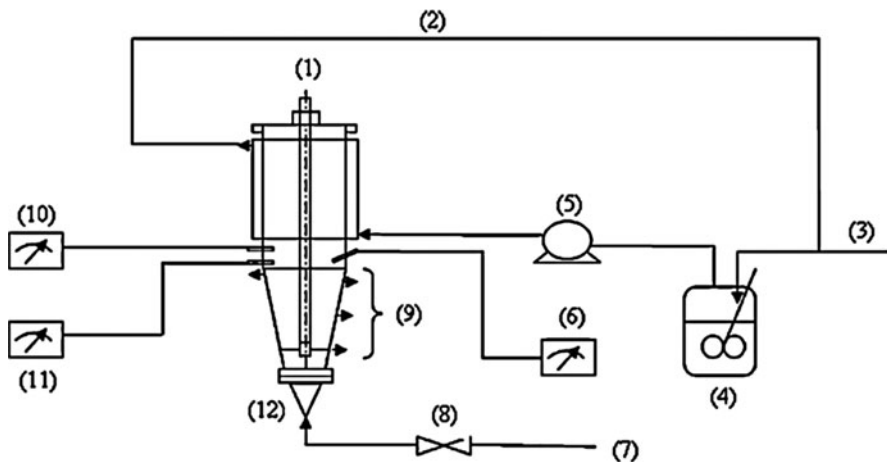
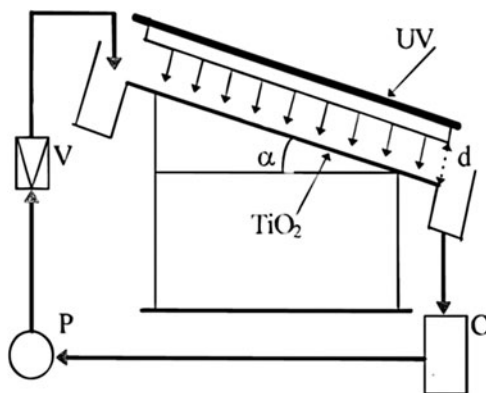


Fig. 16.6 The schematic of the annular photocatalytic reactor system: (1) UV light, (2) recirculation water line, (3) fresh cool water line, (4) cooling water vessel, (5) cooling water pump, (6) temperature meter, (7) compressed air supply line, (8) compressed air regulation valve, (9) sampling ports, (10) pH meter, (11) dissolved oxygen meter, and (12) photoreactor [43]

for continuous operation. This can be achieved by conventional sedimentation [46], cross-flow filtration [47], or membrane filtrations [48, 49]. But the optimal operating parameters are still under investigation [7]. For the type 2 reactors, various immobilizers have been tried as revealed in the literature, such as activated carbon [50, 51], mesoporous clays [52], fibers [53], or membranes [54]. Figure 16.9 shows that anatase  $\text{TiO}_2$  nanoparticles with diameters around 10–20 nm are immobilized on titanate fibers with diameters around 100 nm [53].

**Fig. 16.7** The schematic of the flow-through photoreactor system. *C* container, *P* pump, *V* venturi tube, *UV* UV lamps, *d* distance between the lamps and the plate, *TiO<sub>2</sub>* glass plate with immobilized photocatalyst,  $\alpha$  declination angle [44]



Advantages of using  $\text{TiO}_2$  for water disinfection include that  $\text{TiO}_2$  is very stable in water and ingestion of  $\text{TiO}_2$  has low toxicity to human health [4]. One of the most important issues for  $\text{TiO}_2$  disinfection is the impact from the water turbidity caused by the insoluble particles. On the one hand, these particles impede the penetration of UV light due to scattering and absorption [55]. On the other hand, they will also shield target pathogens from inactivation [7]. Normally, the turbidity of the water should be lower than five nephelometric turbidity units (NTU) to ensure the UV light utilization and photocatalytic reaction [56]. This limit could be achieved by prior treatment processes like screening, filtration, sedimentation, coagulation, and flocculation [7].

### 16.2.3 Carbon Nanotubes and Fullerenes

Carbon nanotubes (CNTs) and Fullerenes are two of the most typical carbon-based nanomaterials. They have been known to have cytotoxicity to mammalian cells with the toxicity decreasing from single-walled CNTs to multi-walled CNTs, and to Fullerenes [11, 57]. Recently, a few studies have also shown that these carbon nanomaterials also have antimicrobial capability [10]. Figure 16.10 shows the different cell morphologies of *E. coli* inoculated with or without single-walled carbon nanotubes (~1 nm diameter) [10]. The antimicrobial effect of CNTs are related to both physical interaction and changing the oxidative stress of the environment [10, 58, 59]. It is also reported that direct contact between CNTs and target microorganisms is required to have an inactivation effect [10]. The antimicrobial effect of Fullerenes may be attributed to ROS production [4, 60], but the understanding of the detailed mechanisms is still very limited.

It is very difficult to disperse CNTs in water without functionalizing or adding surfactants like sodium dodecyl benzenesulfate (SDBS), polyvinylpyrrolidone (PVP), or Triton-X [61]. Most of the current studies apply CNTs by coating them on a porous substrate, like a filter, textile or membrane [10, 62–64].

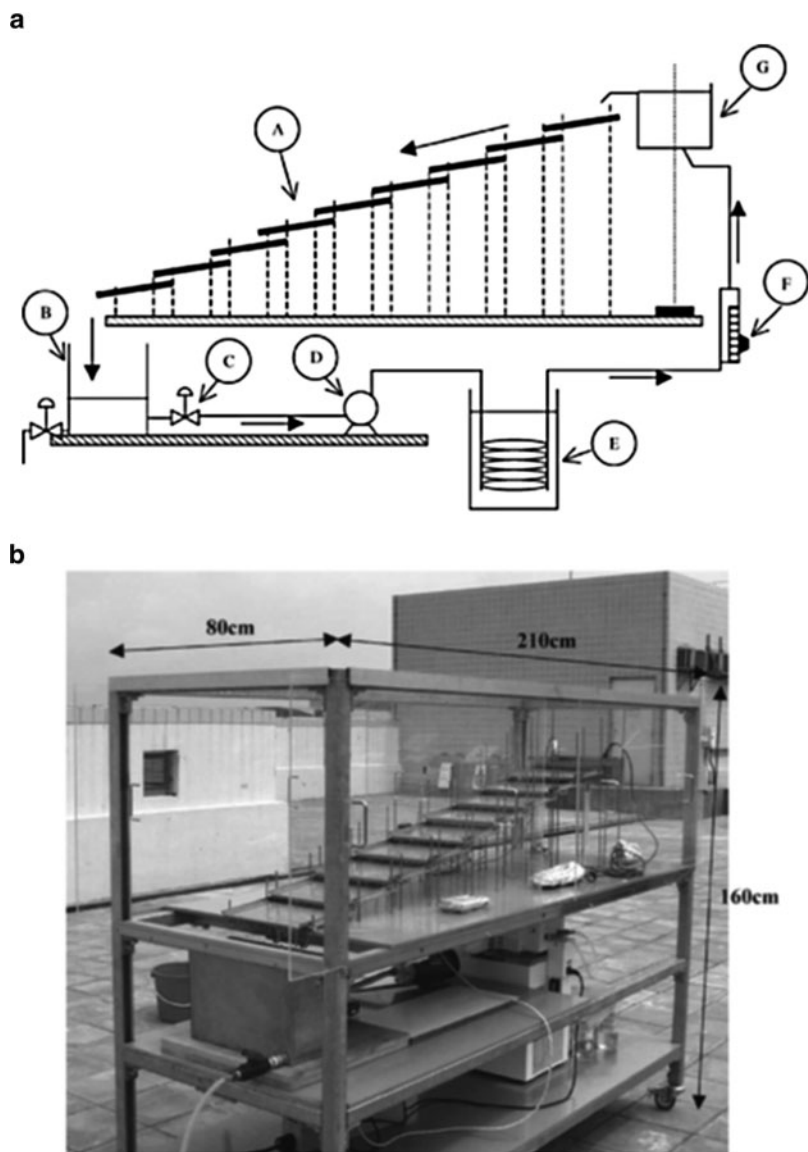


**Fig. 16.8** (a) The schematic of the cascade photoreactor system. *A* TiO<sub>2</sub>-coated plates; *B* tank with drain valve; *C* control; *D* centrifugal pump; *E* cooling coil in water bath; *F* flowmeter; *G* liquid reservoir. (b) Photograph of the pilot scale cascade photoreactor [45]

Fullerenes are also highly insoluble in water [65], but their derivatives can be soluble and still show antimicrobial effects [66]. Fullerenes can also form stable aqueous suspensions as nanoparticles with various particle sizes (Fig. 16.11) [67, 68].



**Fig. 16.9** TEM image of  $\text{TiO}_2$  nanoparticles decorated titanate fibers [53]

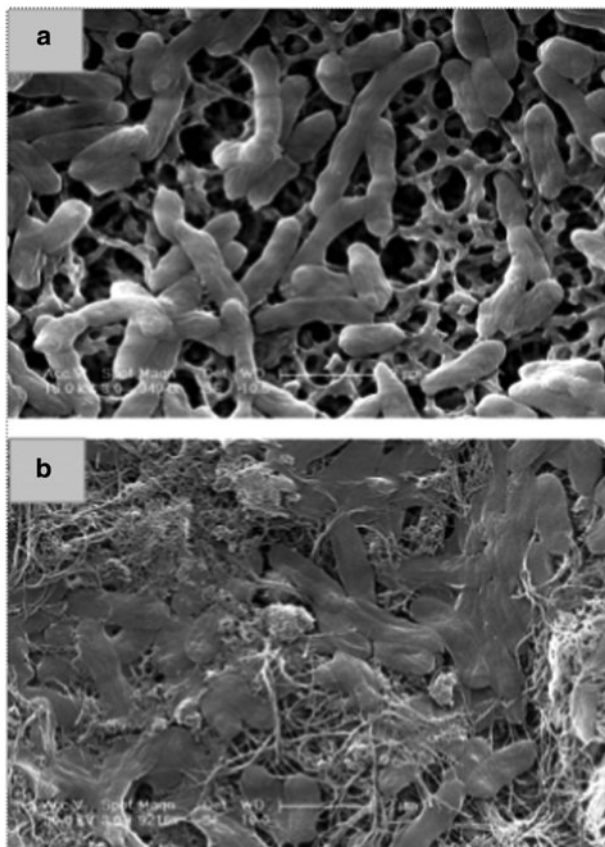
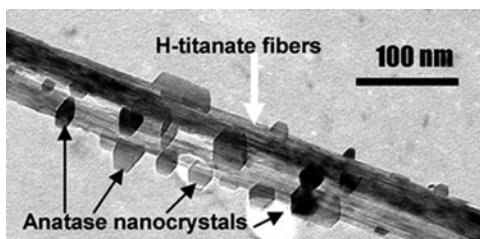


**Fig. 16.10** SEM images of *E. coli*. (a) Cells incubated without SWNTs for 60 min. Cells were filtered and observed via SEM on the filter. (b) Cells incubated with SWNTs for 60 min [10]

### 16.3 Case Studies

Since nanotechnology has introduced new pathways for water disinfection, more and more researchers are investigating new methods for water disinfection using nanomaterials. As introduced in Sect. 16.2, oligodynamic metals, photocatalytic

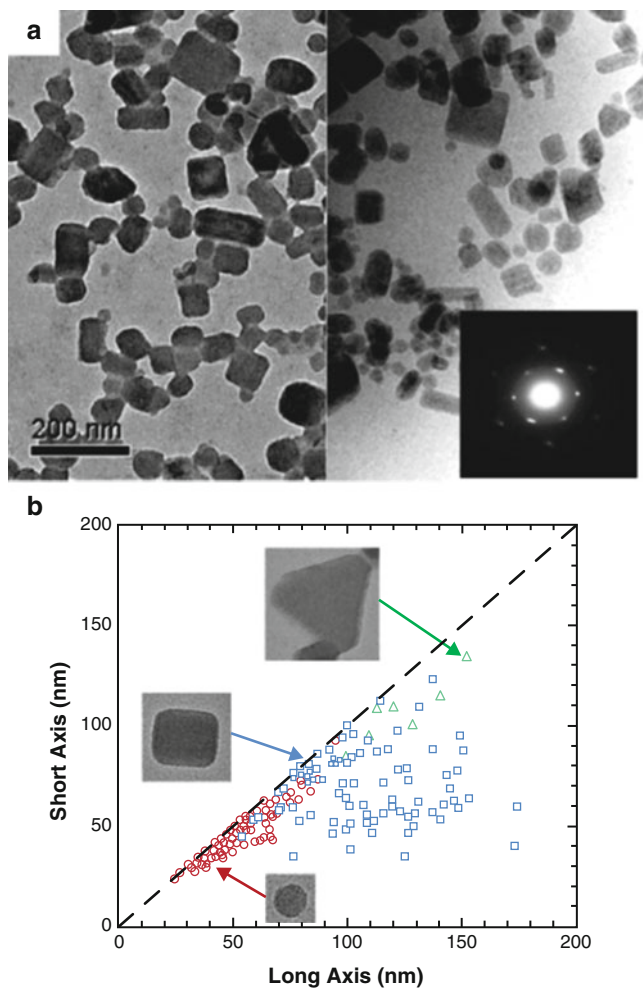


**Fig. 16.11** (a) TEM image of dried (*left*) and flash-frozen (*right*) samples of nano-C60. (b) Particle size and shape distribution. Small aggregates are typically circular in cross-section, intermediate and large ones tending to be rectangular, together with a small fraction of triangular larger particles [68]

semiconductors and some carbon-based materials all have antimicrobial effect. However, their disinfection efficiency depends on a number of factors regarding nanomaterials' unique properties, such as nanomaterial synthesis methods, morphology difference, size difference and how they are used in real treatment devices. Therefore, in terms of large-scale application or commercialization, these nanomaterials need to be used more efficiently and effectively to save materials from synthesis, enhance disinfection efficiency and have lower cost and energy consumption.

In this chapter, we choose six studies carried out by different research groups using antimicrobial material for water disinfection. These studies include the three types of antimicrobial nanomaterials introduced in Chap. 2. Based on these cases, we want to introduce how these nanomaterials are designed and used for water treatment and how nanotechnology is involved in the water disinfection area.

### **16.3.1 Case-1: “TiO<sub>2</sub> Nanotube/CdS Hybrid Electrodes: Extraordinary Enhancement in the Inactivation of *Escherichia coli*”**

Semiconducting materials are of great interest in wastewater treatment and among them TiO<sub>2</sub> is the most promising [69]. Under UV light, TiO<sub>2</sub> enhances the generation of hydroxyl free radicals, with hydrogen ion as a side product. This reaction is useful for bacteria inactivation in water treatment systems because hydroxyl radicals can inactivate bacteria as they will rapidly decimate the organic components of bacteria cells. However, the use of TiO<sub>2</sub> for photocatalytic inactivation of bacteria is limited by its relatively low efficiency of light utilization due to its wide band gap of 3.0–3.2 eV and its poor charge-transfer properties. Hence, the work done by the El-Sayed group introduced a complex system (CdS/TiO<sub>2</sub>) to solve the above two limiting problems in order to increase bacteria inactivation efficiency [70]. And this system lowered the cost of a more complex Pt/CdS/TiO<sub>2</sub> system developed earlier by Kang Q. et al. by removing the high-cost Pt component [71].

They inherited the use of a TiO<sub>2</sub> nanotube (NT) structure developed by Baram et al. [72] for bacteria inactivation. TiO<sub>2</sub> NT arrays were synthesized using immobilized, anodic fabrication [73]. These TiO<sub>2</sub> NT arrays were aligned porous, crystallized, and oriented which made them attractive electron percolation pathways for vectorial charge transfer between interfaces. Moreover, to increase the utilization of visible light, small-band-gap nanocrystal CdS was anchored to this semiconducting metal oxide. CdS nanocrystals was deposited on the crystallized NT surfaces by the successive chemical bath deposition (CBD) method and resulted in enhancement of the charge carrier separation process [74]. SEM images of the materials were shown in Fig. 16.12.

By using this complex CdS/TiO<sub>2</sub> system, they have achieved a better bacteria inactivation in water solution. Two sets of experiments were performed to explore the inactivation efficiency of *E. coli*: one with light only—photochemical, and one with light and applied bias—photoelectrochemical. And to compare the performance of TiO<sub>2</sub>/CdS electrodes, they also used TiO<sub>2</sub> thin films and TiO<sub>2</sub> NT arrays. The schematic diagram of the set-up used for the photochemical and photoelectrochemical is shown in Fig. 16.13. In the photochemical study, electrodes were immersed in separate solutions containing *E. coli* in sulfate buffer under stirring and illumination from a xenon lamp, with a water filter to cut off the IR effect, and samples were collected every 10 min. For the photoelectrochemical study, a two-electrode electrochemical cell was used with the semiconductor material as the

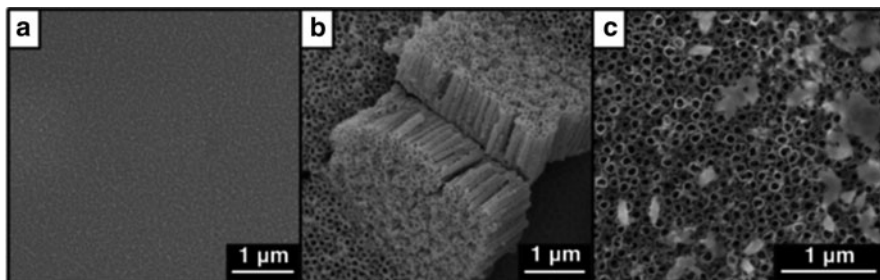
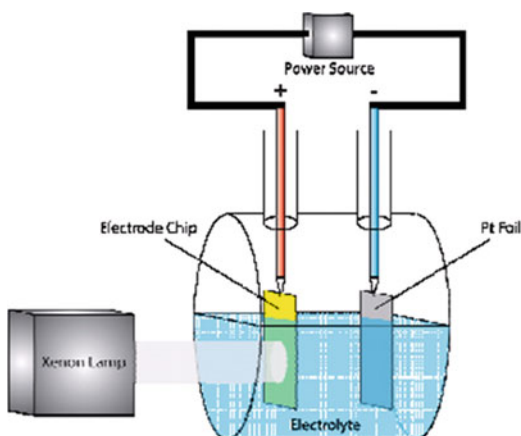


**Fig. 16.12** FESEM images of (a) titania thin film, (b) titanium dioxide nanotubes, and (c) TiO<sub>2</sub>/CdS hybrid electrode [70]

**Fig. 16.13** Schematic diagram of the set-up used for the photochemical and photoelectrochemical disinfection of *E. coli* [70]



working electrode and a Pt foil as the counter electrode under a constant applied potential of 0.5 V. Illumination conditions were the same.

They also measured the diffuse reflectance spectroscopy (DRS)-UV-vis spectra of the three electrodes mentioned above (Fig. 16.14). The TiO<sub>2</sub>/CdS electrode showed an absorption edge red-shifted to 570 nm while the other two electrodes' absorption edges were around 340–380 nm. This shifted absorption edge gave the TiO<sub>2</sub>/CdS electrode a band-gap of 2.17 eV, which means that this hybrid array can harvest visible light.

The results of inactivation were shown as survivability with respect to time (Fig. 16.15). In the photochemical case, the hybrid electrode led to an almost complete inactivation of *E. coli* in only 10 min without any applied bias, which was much higher than both thin film and the pure NT arrays which led to the inactivation of only 40% and 45% of the bacteria, respectively. While with 0.5 V bias to help separate the charge carriers, the hybrid electrode showed an inactivation of *E. coli* in only 3 min.

This disinfection method is very attractive. The complex system of TiO<sub>2</sub> NT/CdS shows a lower band-gap, a higher absorption of visible light and a good charge

**Fig. 16.14** DRS-UV-vis spectra of the three electrodes used to inactivate *E. coli*. CdS greatly increases the visible light absorption capability of the TiO<sub>2</sub> [70]

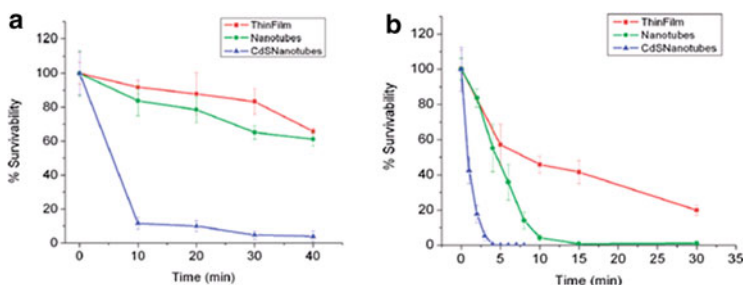
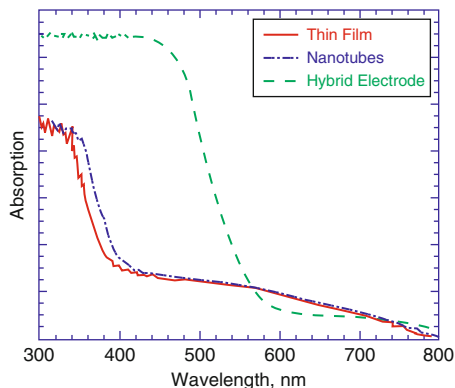


**Fig. 16.15** Inactivation of *E. coli* in photochemical (a) and photoelectrochemical (b) experiments for TiO<sub>2</sub> thin film (red), TiO<sub>2</sub> nanotube array (green), and the hybrid CdS/TiO<sub>2</sub> nanotube array (blue) [70]

transport compared to other TiO<sub>2</sub>-based water disinfection devices. Moreover, the main energy source to support this system is visible light which makes this method clean and of low cost. However, the fabrication process of the hybrid electrode is still relatively complicated compared to other innovative disinfection methods, and the toxicity of cadmium is a big concern. The mechanism of disinfection of this device is by generating hydroxyl free radicals which have high oxidation ability. This method would be more promising in terms of commercialization if the fabrication cost could be further lowered and the cadmium element could be replaced by another non-toxic element.

### 16.3.2 Case-2: “High Speed Water Sterilization Using One-Dimensional Nanostructures”

This work was done by the Cui group at Stanford University [62]. This water treatment device involves both silver nanowires (AgNWs) and carbon nanotubes

(CNTs); however, the disinfection mechanism is claimed not to be just silver disinfection or CNT disinfection. They have developed a high speed electrical assist disinfection device based on a conducting nanotextile. Though the conducting nanotextile is acting like a filter, the disinfection mechanism is not by size exclusion, because the nanotextile has pore sizes of several hundreds of microns which is much larger than the size of bacteria. This device is made through very simple processes and shows a high throughput and low energy consumption for bacteria inactivation in water.

The illustration of filtration set-up and filter fabrication is shown in Fig. 16.16. The filter was made of three components: cotton, CNT and AgNW. Cotton acted as the backbone of the filter since it is cheap, widely available, and chemically and mechanically robust. The conductivity was provided by CNT which was coated onto textile fibers by a simple dipping–drying process. AgNW, which is known to have antimicrobial property, was coated using the same method. AgNWs could form an efficient electrical transport network in filters and they have advantages over Ag nanoparticles (AgNP) in terms of disinfection since they significantly reduce the number of electron hopping times as compared to nanoparticles.

The disinfection idea was based on the fact that noble metal electrodes are known to exhibit antibacterial action under moderate currents, and the enhancement of a sheet of silver nanorods' antibacterial action when placed in an electric field has recently been observed [75, 76]. The experiment set-up was very simple. An external electric field was applied between a nanotextile filter and a counter electrode of copper mesh. Water flowed through the nanotextile filter by gravity force. Bacteria were inactivated while flowing through the nanotextile filter and with the presence of a moderate voltage. Disinfected water was collected from end of the funnel.

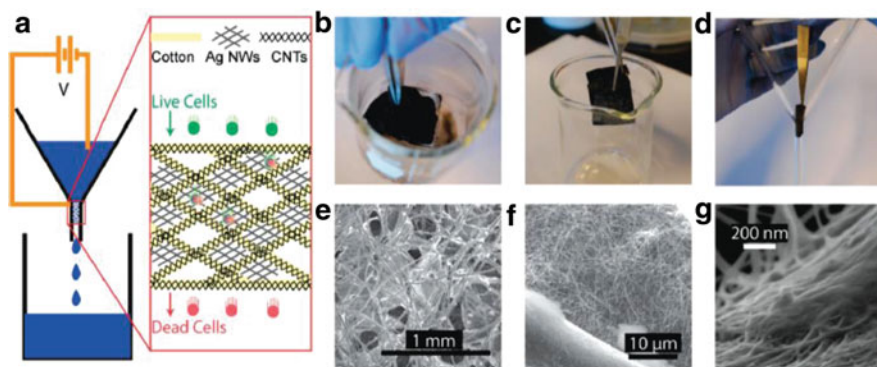
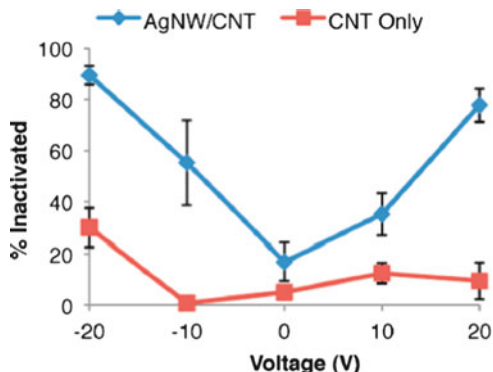


**Fig. 16.16** Schematic, fabrication, and structure of cotton, AgNW/CNT device. (a) Schematic of active membrane device proposed. (b) Treatment of cotton with carbon nanotubes (CNTs). (c) Treatment of device with silver nanowires (AgNWs). (d) Integration of treated cotton into funnel. (e) SEM image showing large scale structure of cotton fibers. (f) SEM image showing AgNWs. (g) SEM image showing CNTs on cotton fibers [62]



**Fig. 16.17** Inactivation efficiency at five biases for AgNW/CNT cotton as well as CNT-only cotton [62]

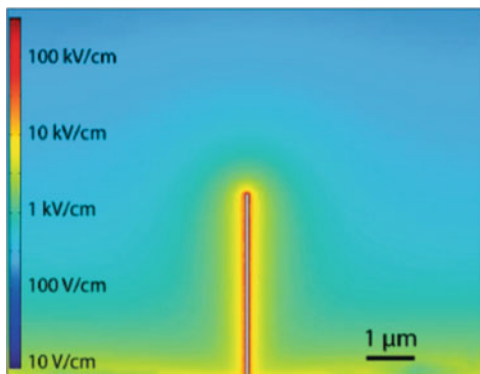


The efficiency of this water disinfection method was studied using *E. coli*. And the results were calculated by counting colonies of both the original bacteria solution and treated water solution cultured on agar plates. From the results, we can see that the AgNW coating can increase disinfection efficiency compared to the filter only with the CNT coating. And with an increased value of external voltage, a higher inactivation efficiency was achieved (Fig. 16.17). The flow rate of this device was 1 L/h and retention time was about 1 s. Moreover, this disinfection method was proved to be effective to different original bacteria concentration from  $10^4$  to  $10^7$  bacteria/mL. The best efficiency of this method reported by the paper was 98% by three times of filtration.

The authors put forward three possible hypotheses which could lead to bacteria inactivation, although the disinfection mechanism was not fully understood yet. The first factor is silver, in this device AgNW. Silver ion and AgNP are known to have antimicrobial properties and are used as coatings in other disinfection applications. In this case, the inactivation effect could be either from  $\text{Ag}^+$  released from oxidized nanomaterial or nanomaterial itself without  $\text{Ag}^+$ . However, the effect of silver cannot alone account for the dramatic improvement of killing efficiency observed when the AgNWs were placed at relatively moderate biases of 20 V. The second hypothesis is that the bacteria were inactivated by the strong external electric field which would cause irreversible electroporation to bacteria cells. By simulation, the electric field near AgNW surface could be as high as tens to hundreds of kilovolts per centimeter (Fig. 16.18). It is known that when electric fields exceeding  $10^5$  V/cm it will adversely affect cell viability by breaking down cell membranes in a process known as electroporation [77]. The third hypothesis is that changes to the solution chemistry during current flow are involved, including pH changes as well as in situ production of chemicals like chlorine, which have also been investigated as a route to sterilizing fluid [78]. Finally, it is also quite possible that two or more of these processes may work together and enhance the inactivation of bacteria.

This electrical assist water disinfection method is very attractive because of its short retention time, low cost of materials used and low energy consumption. And by introducing an external electric field, inactivation efficiency is significantly

**Fig. 16.18** Simulation of e-field near NW surface in solution. Log plot of the electric field near a NW in solution at experimental anodic conditions [62]



improved which reveals that the electric field plays an important role in the bacteria inactivation mechanism. However, there is a health concern when using materials in the nano-sized range. In this chapter, it has been shown that the flow conditions studied did not result in mass material release over the time scales reported. Further work to accurately quantify the amount of material released should be carried out to make this disinfection more promising and capable of being commercialized.

### 16.3.3 Case-3: “Bactericidal Paper Impregnated with Silver Nanoparticles for Point-of-Use Water Treatment”

This work done by the Gray group at McGill University and was aimed to develop a cheap point-of-use water purification device [30]. This filter uses cheap and robust paper as substrate and embed silver nanoparticles in it. The inactivation mechanism of this filter is silver disinfection and the system for water filtration is really simple. Most of the bacteria were in effluent solution after percolation and they were inactivated by AgNPs during percolation as shown in Fig. 16.19.

The paper they used was absorbent blotting paper 0.5 mm thick and weighing 250 g/m<sup>2</sup> (Domtar). AgNPs were deposited by the in situ reduction of silver nitrate on the cellulose fibers of paper. The detailed synthesis process can be found publications by J. He et al. and T. Maneerung et al. [79, 80]. The characterization of the AgNPs on the paper was established by measuring the reflectance spectra of the AgNP with a diffuse reflectance attachment using a UV-vis reflectance spectrum. The shape and size distribution of AgNPs were characterized by electron microscopy (Fig. 16.20). The AgNPs’ size did not relate much to the precursor concentration and all samples of different mass loading of silver showed an average size of  $7.1 \pm 3.7$  nm. With the increase of the precursor silver ion concentration, the silver content on the paper increased, which was also shown by the color change of the sheets. The paper turned darker with response to a higher silver concentration. And a comparison with paper made by soaking into AgNP suspension showed the lowest silver loading on the paper and displayed a gray color (Fig. 16.20).



**Fig. 16.19** Schematic illustration of bacteria percolation through AgNP paper [30]

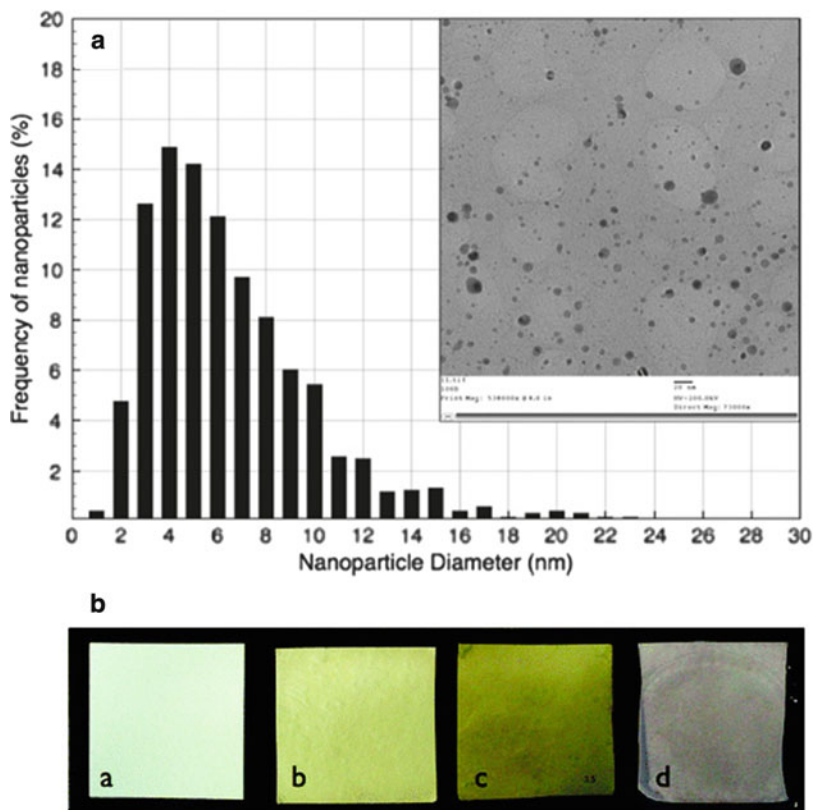
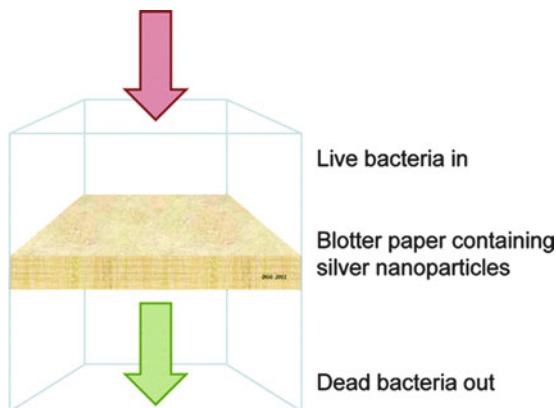


**Fig. 16.20** (a) The distribution of silver nanoparticle diameters, as measured from a TEM image of AgNP on unstained paper fibers removed from sheet (*inset*, scale bar 20 nm). (b) Blotter papers (a) untreated and with silver nanoparticles, (b) 0.2 mg Ag/g paper, (c) 5.8 mg Ag/g paper, and (d) sheet soaked in preformed nanoparticle suspension, 0.06 mg Ag/g paper (each sheet is  $6.5 \times 6.5$  cm) [30]

The bactericidal effectiveness of AgNP paper was evaluated by adding isolated effluent bacteria to agar plates and counting colonies. Two kinds of bacteria *E. coli* (Gram-negative) and *Enterococcus faecalis* (Gram-positive) were tested. The results are shown in Fig. 16.21. Paper prepared with AgNP suspensions showed a lower efficiency than in situ AgNP paper which achieved log-7.6 and log-3.4 removal efficiency of *E. coli* and *E. faecalis* bacteria. And for all the cases, Gram-positive bacteria *E. faecalis* constantly showed a lower efficiency of inactivation.

Considering potential health issue from AgNPs, the authors have analyzed the silver concentration in the effluent water. Graphite furnace atomic absorption was used to measure the total silver concentration including both silver ions and AgNP. The average content of silver was 0.048 ( $\pm 0.018$ ) ppm in the effluent water which meets the US EPA guideline for drinking water of less than 0.1 ppm. However, AgNP suspension-soaked paper showed a higher concentration of silver content in the effluent water.

The mechanism of this method of water purification was silver inactivation of bacteria during percolation. Though the difference of inactivation effect by silver ions or by AgNP can hardly be analyzed, the TEM images of bacteria cells after inactivation showed some morphology changes which are similar to that of bacteria treated with AgNO<sub>3</sub> solution (Fig. 16.22).

This in situ synthesized AgNP paper shows great potential of easily transported and deployed use for emergency or outdoor activities. The bacteria removal efficiency is quite promising. However, the flow rate of 10 mL/min is not high enough compared to other treatment methods such as a ceramic/AgNP filter which has a flow rate of around 25 mL/min. And because of the natural properties of paper, the life time of this filter would not be very long which makes the in situ synthesis seem

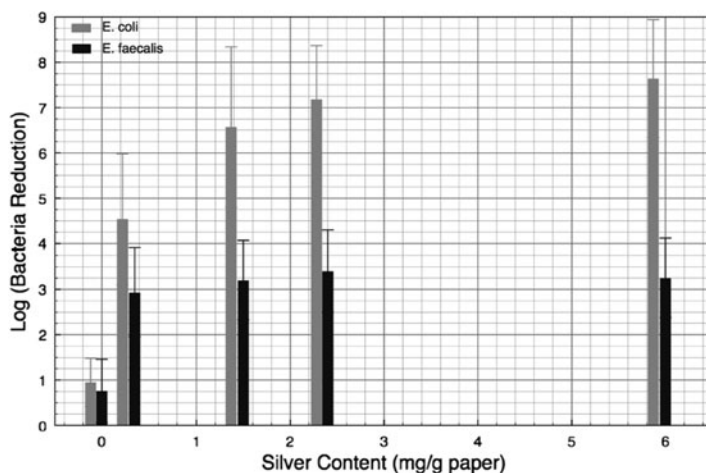


**Fig. 16.21** Log reduction of *E. coli* and *E. faecalis* bacterial count after permeation through the silver nanoparticle paper, at different silver contents in paper. Initial bacterial concentration, 109 CFU/mL (log 9). Error bars standard deviation [30]

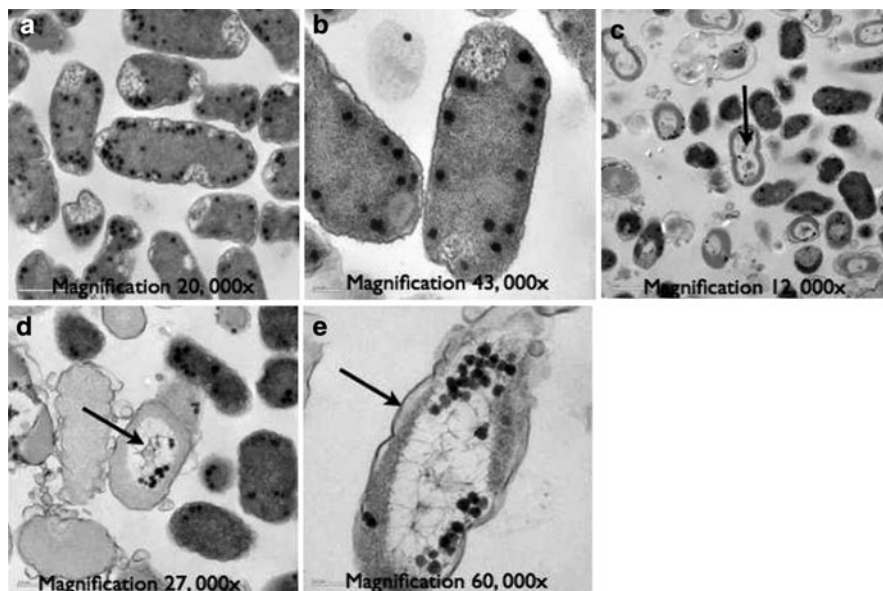


**Fig. 16.22** Internal structure of *E. coli* bacteria imaging by TEM, following percolation experiments. (a, b) control paper (no silver). After exposure to Ag NP paper (c) low electron density region (*arrow*) in the centers of the cells. (d) Condensed form of DNA (*arrow*) in the center of the low electron density region. (e) A gap between the cytoplasm membrane and the cell wall (*arrow*); the cell wall shows serious damage. *Black dots* are not AgNP, but electron dense granules typical of *E. coli* [30]

a little bit complicated if this paper filter is designed for one-time use. But if the life time of this paper-based filter could be increased, this would be very attractive for commercialization.

#### 16.3.4 Case-4: “Electrochemical Multiwalled Carbon Nanotube Filter for Viral and Bacterial Removal and Inactivation”

Carbon nanotubes have been reported to have an inherent antimicrobial activity [10]. Both single-walled carbon nanotube (SWNT)- and multiwalled carbon nanotube (MWNT)-based microfilters have been used for water disinfection to remove bacteria by a sieving mechanism. In addition, the conductive nature of carbon nanotubes allows the introduction of electrochemistry during filtration which could enhance the inactivation efficiency of pathogens in water. The work shown below was done by the Elimelech group at Yale University [63]. They took the advantages of porous and conductive properties of MWNT and made a filter functioning both by size screening and electrochemical disinfection with a small applied bias.

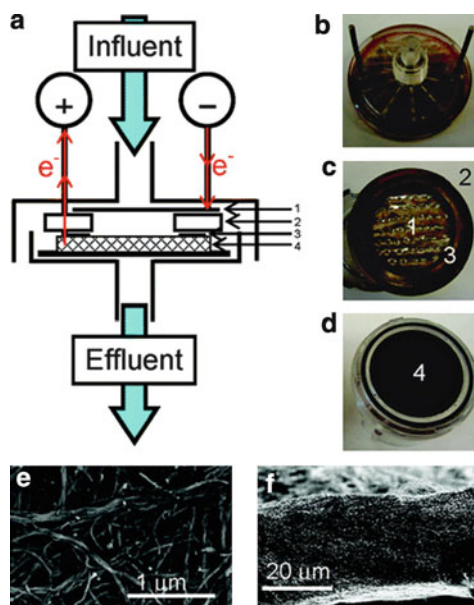


**Fig. 16.23** Electrochemical MWNT filter design and characterization. (a) Depiction of modified electrolytic MWNT filtration setup, where 1 is the perforated stainless steel cathode, 2 is the insulating seal, 3 is the anodic titanium ring connector to the MWNT, and 4 is the anodic MWNT filter. (b) Top view of the modified upper piece of the Millipore filtration apparatus with anodic (*left*) and cathodic (*right*) connectors. (c) View of the upper piece of the filtration apparatus showing the perforated stainless steel cathode. (d) MWNT filter composed of 3 mg MWNTs ( $0.31 \text{ mg/cm}^2$  coverage) on a Teflon membrane ( $5 \text{ }\mu\text{m}$  pore size) on the bottom piece of apparatus. (e) SEM aerial image of the MWNT filter. (f) SEM cross-section (*side*) image of the MWNT filter [63]

The filter design and operation is shown in Fig. 16.23. The MWNT filter was made by filtering MWNT solution onto a  $5\text{-}\mu\text{m}$  PTFE membrane and the mass loading was  $0.31 \text{ mg/cm}^2$ . The average pore diameter was  $93 \pm 38 \text{ nm}$  and the thickness of the MWNT filter was  $22 \pm 2 \text{ }\mu\text{m}$ . The cathode was stainless steel which was on top of the anode CNT filter. An external voltage of 1–3 V was applied during filtration. Both inactivation of viruses (MS2) and of bacteria (*E. coli*) were studied.

The inactivation results showed that, after dispersing effluent water on to an agar plate, no bacteria colonies were formed. All bacteria were removed by the sieving mechanism using the  $\sim 100\text{-nm}$  MWNT filter. And since MR2 virus sizes were much smaller, they measured the virus removal efficiency in effluent water according to bias change (Fig. 16.24). The bacteria and virus adsorbed onto the filter were also investigated. Viability was studied with different bias and exposure time. The experimental result is also shown in Fig. 16.24.

The mechanism of this disinfection method is that at low electric bias, 1–2 V, the dominant inactivation mechanism was direct oxidation by MWNT while at high bias, 3 V, bacteria and virus could be inactivated by indirect oxidation. Their

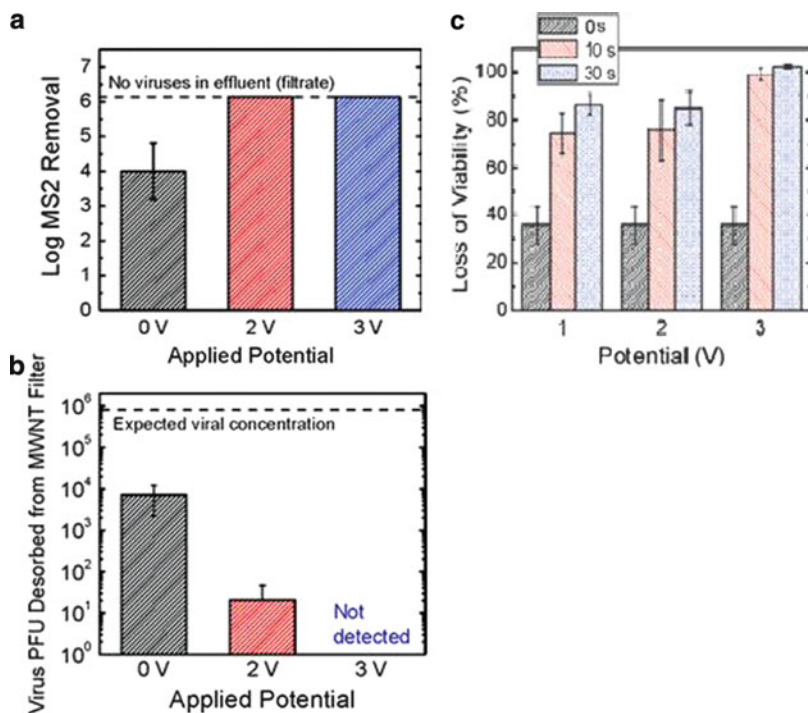


**Fig. 16.24** Electrochemical MS2 removal and/or inactivation versus potential. (a) Log MS2 removal as a function of applied potential during filtration. In fluent was 10 mL of 10 mM NaCl (pH 5.7) and 106 viruses mL<sup>-1</sup> and was filtered at a rate of 4 mL min<sup>-1</sup> (filter approach velocity of 250 L m<sup>-2</sup> h<sup>-1</sup>). Note that at 2 and 3 V, no viruses were detected in the filter effluent. (b) PFU of MS2 adsorbed on MWNT filter as a function of the post filtration applied potential. In fluent was 10 mL of 10 mM NaCl (pH 5.7) with 106 virus mL<sup>-1</sup> and was filtered at a rate of 4 mL min<sup>-1</sup> (filter approach velocity of 250 L m<sup>-2</sup> h<sup>-1</sup>) in the absence of potential. Adsorbed viruses were then electrolyzed for 30 s at 2 or 3 V. (c) Electrochemical loss of *E. coli* viability versus potential and time. *E. coli* suspension [107 cells, (NaCl) = 10 mM, pH 5.7] first sieved onto the MWNT filter and then electrolyzed at an applied voltage of 1, 2, or 3 V for 10 or 30 s. Bacteria were stained immediately after electrolysis for viability assay. Each data point represents the mean of at least duplicate measurements at the same experimental conditions, with error bars representing standard deviations [63]

hypothesis was that at high bias, free radicals would form from electrolyte and oxidized pathogens. And in effluent water, bacteria were removed by the sieving mechanism and the virus was removed by both sieving and electrochemical inactivation.

This disinfection method shows a very effective inactivation of both bacteria and virus, and the filter fabrication is not complicated. However, limited by the small pore sizes of the MWNT filter, the flow rate can only achieve 4 mL/min. And by using the MWNT filter, there are still safety concerns of effluent water quality for point-of-use disinfection.

### 16.3.5 Case-5: “Converting Visible Light into UVC: Microbial Inactivation by $\text{Pr}^{3+}$ -Activated Upconversion Materials”

This work done by the Kim group at Georgia institute of Technology who reported a light-activated antimicrobial surface composed of lanthanide-doped up-conversion luminescent nano- and microcrystalline  $\text{Y}_2\text{SiO}_5$  [81]. This method, unlike that using  $\text{TiO}_2$  which relies on photocatalytically-generated free radicals for disinfection, has a pure optical mechanism and this work is very innovative to use electromagnetic energy for disinfection purposes. This antimicrobial surface can absorb visible light and convert it into Germicidal UVC radiation (Fig. 16.25). Hence, the disinfection mechanism is similar to UV disinfection.

The surface antimicrobial effect was analyzed by studying the inactivation kinetics of *Bacillus subtilis*. Bacteria was deposited and dried on the coated surfaces. The reason this experiment can be carried out in dry condition is because the spores of this organism can remain viable in dry conditions [82]. The results are shown in Fig. 16.26. The sample with  $\text{Pr}^{3+}$ ,  $\text{Gd}^{3+}$  and  $\text{Li}^+$  showed the best performance and inactivation efficiency which could be enhanced by increasing light intensity and exposure time.

This method is innovative for a disinfection mechanism. The inactivation efficiency is relatively low compared to other methods since the group used the lowest excitation intensity to just evaluate the antimicrobial effect brought about by up-conversion materials. Although this technology has not been used in water solution systems, it demonstrates the potential of disinfection and further usage in the water disinfection area. So far, the kinetics is much slower than other methods; however, there is still room for this technology to improve.

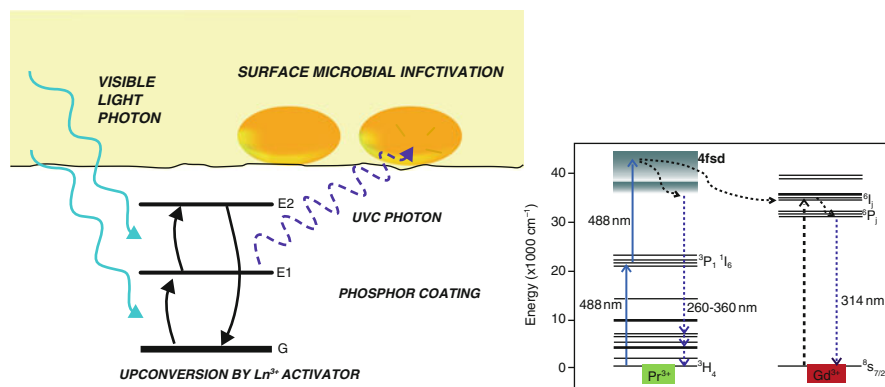


**Fig. 16.25** Utilization of visible-to-ultraviolet upconversion phosphor coating for light-activated antimicrobial materials. The energy diagram depicts excited-state absorption of visible light from the ground-state configuration, G, to the excited states, E1 and E2, to emit a UVC photon upon relaxation (left). Up-conversion mechanisms of  $\text{Pr}^{3+}$  and  $\text{Gd}^{3+}$  UV emissions. Solid blue line shows visible light absorption; dotted black line shows nonradiative energy transfer; dotted purple line shows UV photon emission (right) [81]



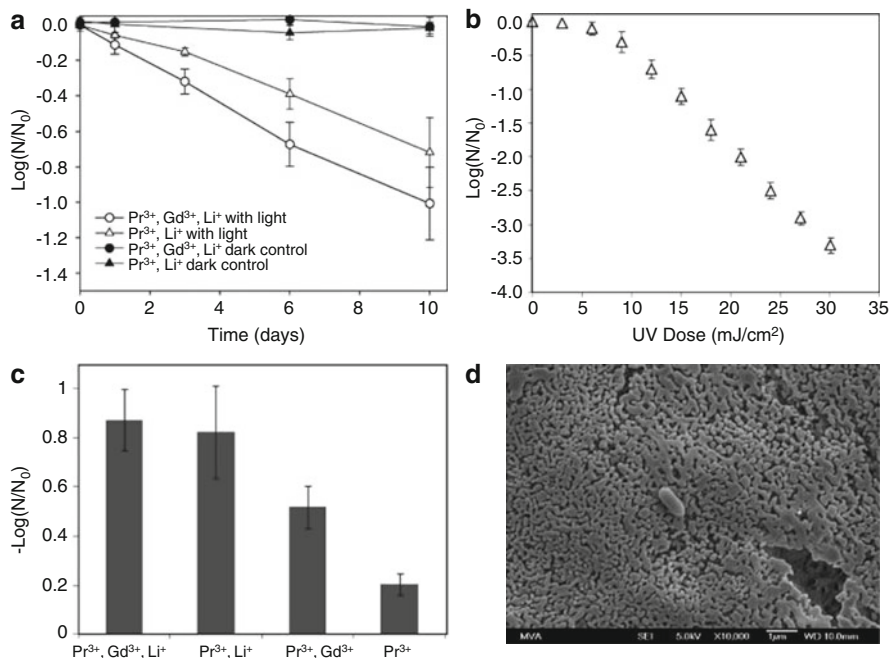


**Fig. 16.26** Inactivation of *Bacillus subtilis* spores on dry phosphor-coated surfaces. (a) Inactivation kinetics of Y<sub>2</sub>SiO<sub>5</sub> phosphors with different doping schemes exposed to “daylight” fluorescent lighting and dark controls. Unactivated surfaces showed no inactivation under visible light after 10 days (data not shown). (b) Inactivation dose–response of *B. subtilis* spores on dry surface exposed to known doses of UVC from low-pressure Hg bulbs,  $\lambda = 254$  nm. The linear portion of this curve was used for biosimetric estimation of the upconversion efficiency of coated samples. (c) 10-day log inactivation of spores on Y<sub>2</sub>SiO<sub>5</sub>-coated surfaces with different doping schemes under visible light. (d) Scanning electron micrograph of a *B. subtilis* spore on a Y<sub>2</sub>SiO<sub>5</sub>: Pr<sup>3+</sup>, Li<sup>+</sup> + nanocrystalline surface prepared through dip-coating in precursor sol solution. White scale bar 1 μm. All error bars standard deviations [81]

### 16.3.6 Case-6: “Sustainable Colloidal-Silver-Impregnated Ceramic Filter for Point-of-Use Water Treatment”

The Colloidal-Silver-Impregnated Ceramic Filter is one of the most representative examples of a commercialized water disinfection product using nanotechnology. In the late 1980s and early 1990s, ceramic filters were already appearing in third world markets; however, the price of those filters were too expensive for local people to afford in the long term. A U.S.-based nongovernmental organization (NGO) called Potters for Peace has developed a new method to fabricate these ceramic filters and has taught this method to local people. The filters look like ceramic pots and in operation they are put into a plastic container (Fig. 16.27). Ceramic filters can removal pathogens by size exclusion, and addition of colloidal silver particles to these filters will enhance the inactivation efficiency because of silver’s antimicrobial properties.



Fig. 16.27 A ceramic filter

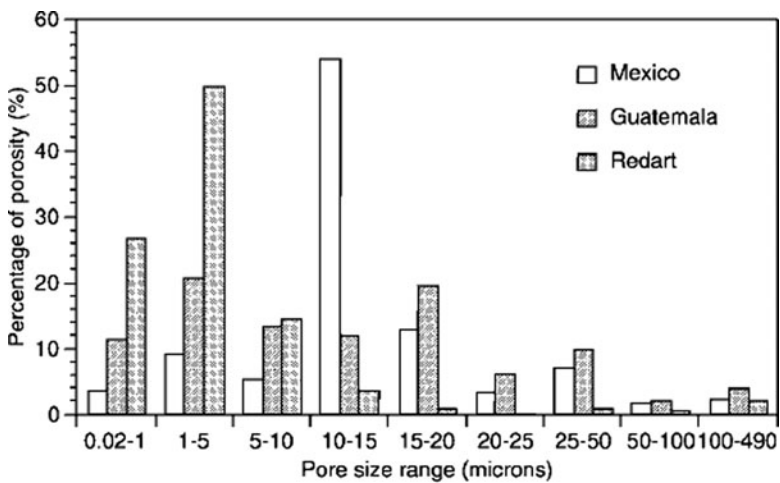
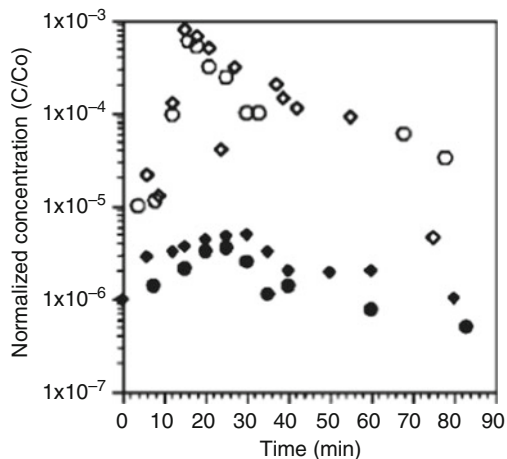


Fig. 16.28 Pore-size distribution for ceramic filters fabricated using Redart, Guatemalan, and Mexican soils [22]

V.A. Oyanedel-Craver and J.A. Simth at the University of Virginia fabricated this kind of ceramic filters using the same method as NGO and tested their performance in laboratory [22]. Filters made of three different soil samples were studied. The porosity study showed similar pore sizes for these three filters (Fig. 16.28). This means that ceramic filters could be fabricated by local labor and the transportation properties of the filters using different raw materials would not differ by very much.





**Fig. 16.29** Effluent *E. coli* concentrations normalized to the influent pulse concentration as a function of time for ceramic filters fabricated with Redart soils without colloidal silver ( $\diamond$  and  $\circ$ ), and painted with ( $\blacklozenge$ ) and submerged in a 600-mg/L colloidal silver solution ( $\bullet$ ) [22]

To improve the efficiency of ceramic filters, colloidal silver nanoparticles were added. This was done by either painting them or submerging them using AgNPs suspensions. After saturation, bacteria removal experiments were done using ceramic filters both with and without silver colloidal particles. The results showed that silver nanoparticles can significantly improve bacteria removal efficiency (Fig. 16.29). And the methods used to adding AgNPs did not influence the efficiency very much, which proves the ease of commercialization of this Colloidal-Silver-Impregnated Ceramic Filter.

The Colloidal-Silver-Impregnated Ceramic Filter is very effective for point-of-use water treatment especially for the third world countries, because it is easy for it to be made by local labor and is of relatively low cost. This method provides a way to protect people in water-stressed areas from water borne diseases.

## 16.4 Challenges and Outlooks

Although antimicrobial nanomaterials have shown promising potential for water disinfection, several challenges still exist for large-scale practical applications.

1. Usually, the synthesis of nanomaterials includes several complex procedures and the scale-up is still challenging, meaning that the cost of the antimicrobial nanomaterials is still a concern based on current technology. Drinking water is essential for everyday life, but most of the antimicrobial nanomaterials are still not affordable for most people for daily use. The most commercialized ceramic filter as discussed previously costs about US\$ 25 each. However, this is still too

- expensive for the people living in some developing countries who do not have safe drinking water access and who need POU disinfection techniques the most urgently.
2. We gain benefit from the antimicrobial effect of the nanomaterials by obtaining safe drinking water without pathogens. However, if these nanomaterials are discharged into the natural environment, they may also kill the microbes that are useful or even essential for the ecosystem. In addition, high concentrations of antimicrobial nanomaterials in the drinking water may also be harmful to human health [71]. Therefore, retaining the antimicrobial nanomaterials in the system is extremely important.
  3. The antimicrobial effect of the nanomaterials is relevant to their high surface-to-volume ratio. Thus, smaller sizes will be preferable. However, smaller sizes will also cause more serious aggregation problems. It will also be more challenging to retain smaller nanomaterials in the system, no matter if it is a sedimentation process or a filtration process.
  4. Since the antimicrobial nanomaterials are required to be retained in the treatment unit, no residual antimicrobial effects can be provided. It will be fine for POU applications, but will be a problem for remote applications with long-distance transport.
  5. Most of the current studies on antimicrobial nanomaterials are conducted in a relatively clean solution [4]. The effects of the natural water qualities are still not well understood and many more studies on real application are required.

## References

1. UNESCO, *Water a shared responsibility*, United Nations Educational, Scientific and Cultural Organization. Scientific and Cultural Organization. Paris, France: UNESCO; New York: Berghahn Books, 2006. p. 20–24.
2. Wolff, G., et al., *The biennial report on freshwater resources*, Washington, D.C., in *the world's water 2006–2007 the biennial report on freshwater resources*. Washington, DC: Island Press, 2006. p. 1–28.
3. WHO, *Water, sanitation and hygiene links to health*. 2004, World Health Organization. [http://www.who.int/water\\_sanitation\\_health/publications/factsfigures04/en/](http://www.who.int/water_sanitation_health/publications/factsfigures04/en/)
4. Li, Q., et al., *Antimicrobial nanomaterials for water disinfection and microbial control: Potential applications and implications*. Water Research, 2008. **42**(18): p. 4591–4602.
5. Diallo, M., et al., *Nanotechnology applications for clean water*. Norwich, NY: William Andrew, 2009. p. 3–15.
6. Nangmenyi, G. and J. Economy, *Nanometallic particles for oligodynamic microbial disinfection*, in *Nanotechnology Applications for Clean Water*, N. Savage, et al., Editors. 2009, William Andrew Inc.: Norwich. p. 3–15.
7. Chong, M.N., et al., *Recent developments in photocatalytic water treatment technology: A review*. Water Research, 2010. **44**(10): p. 2997–3027.
8. Gondal, M.A., M.A. Dastageer, and A. Khalil, *Synthesis of nano-WO<sub>3</sub> and its catalytic activity for enhanced antimicrobial process for water purification using laser induced photo-catalysis*. Catalysis Communications, 2009. **11**(3): p. 214–219.
9. Lee, J.S., et al., *Photochemical and antimicrobial properties of novel C60 derivatives in aqueous systems*. Environmental Science & Technology, 2009. **43**(17): p. 6604–6610.

10. Kang, S., et al., *Single-walled carbon nanotubes exhibit strong antimicrobial activity*. *Langmuir*, 2007. **23**(17): p. 8670–8673.
11. Magrez, A., et al., *Cellular toxicity of carbon-based nanomaterials*. *Nano Letters*, 2006. **6**(6): p. 1121–1125.
12. Russell, A.D. and W.B. Hugo, *Antimicrobial activity and action of silver*. *Progress in Medicinal Chemistry*, 1994. **31**: p. 351–370.
13. Jung, W.K., et al., *Antibacterial activity and mechanism of action of the silver ion in Staphylococcus aureus and Escherichia coli*. *Applied and Environmental Microbiology*, 2008. **74**(7): p. 2171–2178.
14. Inoue, Y., et al., *Bactericidal activity of Ag-zeolite mediated by reactive oxygen species under aerated conditions*. *Journal of Inorganic Biochemistry*, 2002. **92**(1): p. 37–42.
15. Li, W.R., et al., *Antibacterial effect of silver nanoparticles on Staphylococcus aureus*. *Biometals*, 2011. **24**(1): p. 135–141.
16. Morones, J.R., et al., *The bactericidal effect of silver nanoparticles*. *Nanotechnology*, 2005. **16**(10): p. 2346–2353.
17. Pal, S., Y.K. Tak, and J.M. Song, *Does the antibacterial activity of silver nanoparticles depend on the shape of the nanoparticle? A study of the gram-negative bacterium Escherichia coli*. *Applied and Environmental Microbiology*, 2007. **73**(6): p. 1712–1720.
18. Gogoi, S.K., et al., *Green fluorescent protein-expressing Escherichia coli as a model system for investigating the antimicrobial activities of silver nanoparticles*. *Langmuir*, 2006. **22**(22): p. 9322–9328.
19. Larimer, C., et al., *The segregation of silver nanoparticles in low-cost ceramic water filters*. *Materials Characterization*, 2010. **61**(4): p. 408–412.
20. Yaohui, L., et al., *Silver nanoparticle-decorated porous ceramic composite for water treatment*. *Journal of Membrane Science*, 2009. 331(1–2): p. 50–56.
21. van Halem, D., et al., *Assessing the sustainability of the silver-impregnated ceramic pot filter for low-cost household drinking water treatment*. *Physics and Chemistry of the Earth*, 2009. **34**(1–2): p. 36–42.
22. Oyanedel-Craver, V.A. and J.A. Smith, *Sustainable colloidal-silver-impregnated ceramic filter for point-of-use water treatment*. *Environmental Science & Technology*, 2008. **42**(3): p. 927–933.
23. Yang, L., et al., *Development and characterization of porous silver-incorporated hydroxyapatite ceramic for separation and elimination of microorganisms*. *Journal of Biomedical Materials Research Part B-Applied Biomaterials*, 2007. **81B**(1): p. 50–56.
24. Halem, D.v., et al., *Ceramic silver-impregnated pot filters for household drinking water treatment in developing countries: Material characterization and performance study*. *Water Science and Technology: Water Supply*, 2007. **7**(5–6): p. 9–17.
25. Nangmenyi, G., et al., *Synthesis and characterization of silver-nanoparticle-impregnated fibreglass and utility in water disinfection*. *Nanotechnology*, 2009. **20**(49): p. 1–10.
26. Nangmenyi, G., et al., *Bactericidal activity of Ag nanoparticle-impregnated fibreglass for water disinfection*. *Journal of Water and Health*, 2009. **7**(4): p. 657–663.
27. Zhang, X.L., et al., *Immobilizing silver nanoparticles onto the surface of magnetic silica composite to prepare magnetic disinfectant with enhanced stability and antibacterial activity*. *Colloids and Surfaces a-Physicochemical and Engineering Aspects*, 2011. **375**(1–3): p. 186–192.
28. Gangadharan, D., et al., *Polymeric microspheres containing silver nanoparticles as a bactericidal agent for water disinfection*. *Water Research*, 2010. **44**(18): p. 5481–5487.
29. De Gussemé, B., et al., *Virus disinfection in water by biogenic silver immobilized in polyvinylidene fluoride membranes*. *Water Research*, 2011. **45**(4): p. 1856–1864.
30. Dankovich, T.A. and D.G. Gray, *Bactericidal paper impregnated with silver nanoparticles for point-of-use water treatment*. *Environmental Science & Technology*, 2011. **45**(5): p. 1992–1998.

31. Panyala, N.R., E.M. Pena-Mendez, and J. Havel, *Silver or silver nanoparticles: A hazardous threat to the environment and human health?* Journal of Applied Biomedicine, 2008. **6**(3): p. 117–129.
32. USEPA, *National secondary drinking water regulations*. 2002. p. 6. <http://www.epa.gov/ogwdw/consumer/pdf/mcl.pdf>
33. Silver, S., *Bacterial silver resistance: Molecular biology and uses and misuses of silver compounds*. FEMS Microbiology Reviews, 2003. **27**(2–3): p. 341–353.
34. Matsunaga, T., et al., *Photoelectrochemical sterilization of microbial-cells by semiconductor powders*. FEMS Microbiology Letters, 1985. **29**(1–2): p. 211–214.
35. Kikuchi, Y., et al., *Photocatalytic bactericidal effect of TiO<sub>2</sub> thin films: Dynamic view of the active oxygen species responsible for the effect*. Journal of Photochemistry and Photobiology a-Chemistry, 1997. **106**(1–3): p. 51–56.
36. Adams, L.K., et al., *Comparative toxicity of nano-scale TiO<sub>2</sub>, SiO<sub>2</sub> and ZnO water suspensions*. Water Science and Technology, 2006. **54**(11–12): p. 327–334.
37. Collins-Martinez, V., A.L. Ortiz, and A.A. Elguezabal, *Influence of the anatase/rutile ratio on the TiO<sub>2</sub> photocatalytic activity for the photodegradation of light hydrocarbons*. International Journal of Chemical Reactor Engineering, 2007. **5**: A29.
38. Page, K., et al., *Titania and silver-titania composite films on glass-potent antimicrobial coatings*. Journal of Materials Chemistry, 2007. **17**(1): p. 95–104.
39. Kim, J.P., et al., *Manufacturing of anti-viral inorganic materials from colloidal silver and titanium oxide*. Revue Roumaine De Chimie, 2006. **51**(11): p. 1121–1129.
40. Wei, C., et al., *Bactericidal activity of TiO<sub>2</sub> photocatalyst in aqueous-media - Toward a solar-assisted water disinfection system*. Environmental Science & Technology, 1994. **28**(5): p. 934–938.
41. Reed, R.H., *The inactivation of microbes by sunlight: Solar disinfection as a water treatment process*. Advances in Applied Microbiology, Vol 54, 2004. **54**: p. 333–365.
42. Blanco, J., et al., *Review of feasible solar energy applications to water processes*. Renewable & Sustainable Energy Reviews, 2009. **13**(6–7): p. 1437–1445.
43. Chong, M.N., et al., *Optimisation of an annular photoreactor process for degradation of Congo Red using a newly synthesized titania impregnated kaolinite nano-photocatalyst*. Separation and Purification Technology, 2009. **67**(3): p. 355–363.
44. Belhacova, L., et al., *Inactivation of microorganisms in a flow-through photoreactor with an immobilized TiO<sub>2</sub> layer*. Journal of Chemical Technology and Biotechnology, 1999. **74**(2): p. 149–154.
45. Chan, A.H.C., et al., *Solar photocatalytic thin film cascade reactor for treatment of benzoic acid containing wastewater*. Water Research, 2003. **37**(5): p. 1125–1135.
46. Fernandez-Ibanez, P., et al., *Application of the colloidal stability of TiO<sub>2</sub> particles for recovery and reuse in solar photocatalysis*. Water Research, 2003. **37**(13): p. 3180–3188.
47. Doll, T.E. and F.H. Frimmel, *Cross-flow microfiltration with periodical back-washing for photocatalytic degradation of pharmaceutical and diagnostic residues-evaluation of the long-term stability of the photocatalytic activity of TiO<sub>2</sub>*. Water Research, 2005. **39**(5): p. 847–854.
48. Zhang, X.W., et al., *TiO<sub>2</sub> nanowire membrane for concurrent filtration and photocatalytic oxidation of humic acid in water*. Journal of Membrane Science, 2008. **313**(1–2): p. 44–51.
49. Zhao, Y.J., et al., *Fouling and regeneration of ceramic microfiltration membranes in processing acid wastewater containing fine TiO<sub>2</sub> particles*. Journal of Membrane Science, 2002. **208**(1–2): p. 331–341.
50. Lee, D.K., et al., *Photocatalytic oxidation of microcystin-LR in a fluidized bed reactor having TiO<sub>2</sub>-coated activated carbon*. Separation and Purification Technology, 2004. **34**(1–3): p. 59–66.
51. Li, Y.J., M.Y. Ma, and X.H. Wang, *Inactivated properties of activated carbon-supported TiO<sub>2</sub> nanoparticles for bacteria and kinetic study*. Journal of Environmental Sciences-China, 2008. **20**(12): p. 1527–1533.
52. Chong, M.N., et al., *Synthesis and characterisation of novel titania impregnated kaolinite nano-photocatalyst*. Microporous and Mesoporous Materials, 2009. **117**(1–2): p. 233–242.

53. Zhu, H.Y., et al., *Hydrogen titanate nanofibers covered with anatase nanocrystals: A delicate structure achieved by the wet chemistry reaction of the titanate nanofibers*. Journal of the American Chemical Society, 2004. **126**(27): p. 8380–8381.
54. Kwak, S.Y., S.H. Kim, and S.S. Kim, *Hybrid organic/inorganic reverse osmosis (RO) membrane for bactericidal anti-fouling. 1. Preparation and characterization of TiO<sub>2</sub> nanoparticle self-assembled aromatic polyamide thin-film-composite (TFC) membrane*. Environmental Science & Technology, 2001. **35**(11): p. 2388–2394.
55. Tang, C. and V. Chen, *The photocatalytic degradation of reactive black 5 using TiO<sub>2</sub>/UV in an annular photoreactor*. Water Research, 2004. **38**(11): p. 2775–2781.
56. Gelover, S., et al., *A practical demonstration of water disinfection using TiO<sub>2</sub> films and sunlight*. Water Research, 2006. **40**(17): p. 3274–3280.
57. Jia, G., et al., *Cytotoxicity of carbon nanomaterials: Single-wall nanotube, multi-wall nanotube, and fullerene*. Environmental Science & Technology, 2005. **39**(5): p. 1378–1383.
58. Kang, S., et al., *Antibacterial effects of carbon nanotubes: Size does matter*. Langmuir, 2008. **24**(13): p. 6409–6413.
59. Narayan, R.J., C.J. Berry, and R.L. Brigmon, *Structural and biological properties of carbon nanotube composite films*. Materials Science and Engineering B-Solid State Materials for Advanced Technology, 2005. **123**(2): p. 123–129.
60. Markovic, Z., et al., *The mechanism of cell-damaging reactive oxygen generation by colloidal fullerenes*. Biomaterials, 2007. **28**(36): p. 5437–5448.
61. Hu, L.B., D.S. Hecht, and G. Gruner, *Carbon nanotube thin films: Fabrication, properties, and applications*. Chemical Reviews, 2010. **110**(10): p. 5790–5844.
62. Schoen, D.T., et al., *High speed water sterilization using one-dimensional nanostructures*. Nano Letters, 2010. **10**(9): p. 3628–3632.
63. Vecitis, C.D., et al., *Electrochemical multiwalled carbon nanotube filter for viral and bacterial removal and inactivation*. Environmental Science & Technology, 2011. **45**(8): pp. 3672–3679.
64. Brady-Estevez, A.S., S. Kang, and M. Elimelech, *A single-walled-carbon-nanotube filter for removal of viral and bacterial pathogens*. Small, 2008. **4**(4): p. 481–484.
65. Heymann, D., *Solubility of fullerenes C-60 and C-70 in seven normal alcohols and their deduced solubility in water*. Fullerene Science and Technology, 1996. **4**(3): p. 509–515.
66. Spesia, M.B., A.E. Milanese, and E.N. Durantini, *Synthesis, properties and photodynamic inactivation of Escherichia coli by novel cationic fullerene C-60 derivatives*. European Journal of Medicinal Chemistry, 2008. **43**(4): p. 853–861.
67. Brant, J.A., et al., *Characterizing the impact of preparation method on fullerene cluster structure and chemistry*. Langmuir, 2006. **22**(8): p. 3878–3885.
68. Fortner, J.D., et al., *C-60 in water: Nanocrystal formation and microbial response*. Environmental Science & Technology, 2005. **39**(11): p. 4307–4316.
69. Zhang, D., G. Li, and J.C. Yu, *Inorganic materials for photocatalytic water disinfection*. Journal of Materials Chemistry, 2010. **20**(22): p. 4529.
70. Hayden, S.C., N.K. Allam, and M.A. El-Sayed, *TiO<sub>2</sub> nanotube/CdS hybrid electrodes: Extraordinary enhancement in the inactivation of Escherichia coli*. Journal of the American Chemical Society, 2010. **132**(41): p. 14406–14408.
71. Kang, Q., et al., *A ternary hybrid CdS/Pt-TiO<sub>2</sub> nanotube structure for photoelectrocatalytic bactericidal effects on Escherichia coli*. Biomaterials, 2010. **31**(12): p. 3317–3326.
72. Baram, N., et al., *Enhanced inactivation of E. coli bacteria using immobilized porous TiO<sub>2</sub> photoelectrocatalysis*. Electrochimica Acta, 2009. **54**(12): p. 3381–3386.
73. Allam, N.K. and C.A. Grimes, *Effect of cathode material on the morphology and photoelectrochemical properties of vertically oriented TiO<sub>2</sub> nanotube arrays*. Solar Energy Materials and Solar Cells, 2008. **92**(11): p. 1468–1475.
74. Allam, N.K., K. Shankar, and C.A. Grimes, *Photoelectrochemical and water photoelectrolysis properties of ordered TiO<sub>2</sub> nanotubes fabricated by Ti anodization in fluoride-free HCl electrolytes*. Journal of Materials Chemistry, 2008. **18**(20): p. 2341.

75. Spadaro, J.A., et al., *Antibacterial effects of silver electrodes with weak direct current*. *Antimicroblal Agents and Chemotherapy*, 1974. **6**(5): p. 637–642.
76. Akhavan, O. and E. Ghaderi, *Enhancement of antibacterial properties of Ag nanorods by electric field*. *Science and Technology of Advanced Materials*, 2009. **10**(1): p. 015003.
77. Tsong, T.Y., *Electroporation of cell-membranes*. *Biophysical Journal*, 1991. **60**: p. 297–306.
78. Li, X.Y., et al., *Electrochemical disinfection of saline wastewater effluent*. *Journal of Environmental Engineering*, 2002. **128**(8): p. 697–704.
79. He, J., T. Kunitake, and A. Nakao, *Facile in situ synthesis of noble metal nanoparticles in porous cellulose fibers*. *Chemistry of Materials*, 2003. **15**(23): p. 4401–4406.
80. Maneerung, T., S. Tokura, and R. Rujiravanit, *Impregnation of silver nanoparticles into bacterial cellulose for antimicrobial wound dressing*. *Carbohydrate Polymers*, 2008. **72**(1): p. 43–51.
81. Cates, E.L., M. Cho, and J.-H. Kim, *Converting visible light into UVC: Microbial inactivation by Pr<sup>3</sup> + -activated upconversion materials*. *Environmental Science & Technology*, 2011, **45**(8): p. 3680–3686. doi: [10.1021/es200196c](https://doi.org/10.1021/es200196c)
82. Nicholson, W.L. and B. Galeano, *UV resistance of Bacillus anthracis spores revisited: Validation of Bacillus subtilis spores as UV surrogates for spores of B. anthracis Sterne*. *Applied and Environmental Microbiology*, 2003. **69**(2): p. 1327–1330.